

Surface conduction and length scales in porous media

Jayanth R. Banavar

Schlumberger-Doll Research, Ridgefield, Connecticut 06877-4108

Marek Cieplak*

Department of Physics and Astronomy, Johns Hopkins University, Baltimore, Maryland 21218

David Linton Johnson†

Schlumberger-Doll Research, Ridgefield, Connecticut 06877-4108

(Received 20 November 1987; revised manuscript received 9 February 1988)

Transport in porous media is studied using renormalization-group methods with particular emphasis on surface conduction and the determination of a measure of the characteristic length scale of dynamically connected pores. The nonlinear behavior of the conductivity as a function of pore fluid conductivity increases with the sinuosity of the pores. The nonuniversal critical behavior of the transport at the percolation threshold for power-law pore size distributions is studied.

Porous media, such as sedimentary rocks, catalytic beds, and biological cells play an important role in many disciplines.¹ In general, transport in porous media is controlled by the pore size distribution and their connectivity. Renormalization-group (RG) techniques have proved to be valuable for studying problems with many length scales. In particular, the hierarchical lattices, whose basic units are shown in Fig. 1, are amenable to a simple RG analysis and mimic a cubic lattice in $d=3$ and the percolation backbone in $d=4$. We use these lattices to study transport in porous media with an emphasis on surface conduction and the elucidation of the Λ parameter,²⁻⁵ a length scale characterizing fluid transport. We show that the electrical conductivity of a sample with fixed surface conductivity Σ is a nonlinear function of pore fluid conductivity σ_f when the pore space is sinuous. For these models we show that Λ is still the relevant size parameter for fluid flow permeability. Further, using the hierarchical model⁶ for the percolation backbone and scaling theory,⁷ we study the *nonuniversal* critical behavior of the

conductivity, permeability, and the Λ parameter at $p=p_c$; the exponents depend on the probability distribution (PD) of pore radii $P(r)$ in the $r \rightarrow 0$ limit.

Consider a porous medium in which fluid-filled pores form a connected network embedded in an insulator. The electrical conductivity of the medium σ is proportional to σ_f and it depends on the porosity (the volume fraction of the conducting phase). The permeability k , is a fluid-transport analog of σ . It is defined by the Darcy equation $\mathbf{v} = -(k/\eta)\nabla P$, where \mathbf{v} is the fluid flow velocity, η is the viscosity, and ∇P is the pressure gradient across the medium. On changing all pore and grain sizes by a factor b , k changes by a factor b^2 unlike σ , which is scale invariant.

The electrical conductivity of the porous medium is obtained by solving Poisson's equation in the pore space. Following Ref. 2, the dynamically connected pore sizes can be characterized by means of a geometrical pore-size parameter Λ , which may be determined by computing σ in the presence of an additional pore surface conductivity Σ . Such surface conductivity arises in shaly rocks, due to clay minerals which coat the pore-grain interface.^{8,9} When the bulk conduction due to σ_f dominates the surface conduction, perturbation theory yields

$$\lim_{\Sigma \rightarrow 0} \sigma(\sigma_f, \Sigma) = \sigma(\sigma_f, \Sigma=0) \left[1 + \frac{2\Sigma}{\Lambda\sigma_f} + O(\Sigma^2) \right]. \quad (1)$$

In general, $2/\Lambda = \int |E_0|^2 ds / \int |E_0|^2 dV_p$, where E_0 is the microscopic electric field when $\Sigma=0$, the numerator is integrated over the pore-wall surface and the denominator over the pore volume. Λ is well defined for any porous medium and describes the effects of an internal boundary layer in a variety of situations such as the shaly rock problem, high-frequency viscous damping of acoustic waves, and healing length effects in fourth sound. It has been shown²⁻⁵ in various situations that Λ may also provide a measure of the length scale related to k ,

$$k = c\Lambda^2/8F, \quad (2)$$

where $F = \sigma_f/\sigma(\sigma_f, \Sigma=0)$ and c is a number of order uni-

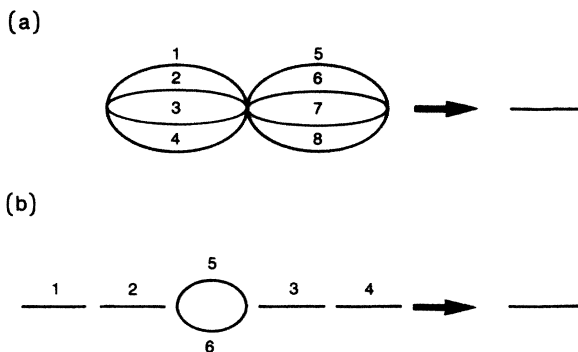


FIG. 1. Hierarchical models for (a) $d=3$ cubic lattice and (b) the percolation backbone in $d=4$. [The number of singly connected bonds in the basic unit is $8/(6-d)$, $2 \leq d \leq 6$.] At each level of the iteration, every bond is replaced by the basic unit on the left.

ty. Simulations of a model periodic porous medium,² calculations of periodic arrays of *charged* spheres in an electrolyte,⁹ and experiments on rocks⁸ show curvature in the σ vs σ_f plot. On the other hand, analytic calculations⁴ on network models of porous media using effective medium theory and percolation ideas yield nearly linear behavior. We show that the curvature can arise due to geometric effects when the surface conduction paths are different from the bulk conduction paths. The nonlinear dependence of σ on σ_f for nonzero values of Σ is important when deducing the properties of shaly rocks.

Consider, first, a cylindrical pore of radius r and length l . The electrical conductance is given by

$$g_e = \frac{\pi r^2}{l} \sigma_f \left(1 + \frac{2}{r} \frac{\Sigma}{\sigma_f} \right)$$

and

$$\sigma = \sigma_f \left(1 + \frac{2}{r} \frac{\Sigma}{\sigma_f} \right).$$

In this case, $\Lambda = r$, $F = 1$, and the σ vs σ_f plot is a straight line. The hydraulic conductance $g_h = (k/\eta)(\pi r^2/l)$ with $k = r^2/8$. g_h is proportional to r^4 . From Eq. (2), $c \equiv 1$.

The conductance of a three-dimensional (3D) network of cylindrical tubes can be estimated using the Migdal-Kadanoff RG scheme¹⁰ illustrated in Fig. 1(a). Each of the bonds represents either an electric conductance, hydraulic conductance, or a Λ value. In practice, a pool of typically 10^5 bonds is constructed for each of these three cases. Eight members of the pool are selected at random and combined to give one member of a new pool. The process is repeated until a new pool of 10^5 bonds is produced. This corresponds to one iteration. For the starting pools given a PD of cylinder radii (the lengths are assumed to be fixed), the Λ 's are equal to the radii, while g_e and g_h are given by the equations in the previous paragraph. The g 's are combined using Kirchoff's laws and the recursion relation for Λ is

$$1/\Lambda' = (a_1 b_2 + b_1 a_2)/(a_2 b_2) - (a_1 + b_1)/(a_2 + b_2),$$

where $a_j = \sum_{k=1}^4 \Lambda_k^j$ and $b_j = \sum_{k=5}^8 \Lambda_k^j$. This relation is obtained by making a small Σ expansion of σ .

For identical pores, Λ is invariant from one iteration to the next, whereas the conductances grow by a factor of 2. The conductivity is obtained on dividing the conductance

after k iterations by 2^k . In the random case, an average is taken over the members of the pool. Convergence is obtained within about 10 iterations. The results are shown in Table I. For a uniform PD of initial radii in the interval $[0,1]$, $\Lambda \approx 0.61$ and $c \approx 1.37$, compared to the effective medium theory result⁴ of $\Lambda \approx 0.51$ and $c \approx 1.46$. (Λ and the radii are in the same units.) In accord with effective medium theory, the σ vs σ_f plot (Fig. 2) obtained by RG techniques, for the 3D network is virtually straight. Replacing each bond by two tubes in series yields only a slight curvature. For these two cases, the bulk and the surface tortuosities are similar.

Real pores are rarely straight tubes. The effects of a sinuous pore (for which the surface and bulk tortuosities are different) may be simulated by combining in series n tubes of fixed length but varying in radii. The ordering of the tubes is irrelevant. The radii were chosen to increase linearly from $r_0 = 0.2$ with increments $\Delta r = 0.2$. Figure 2 shows the conductivity when each sinuous pore is identical and consists of 100 and 1000 subtubes. The larger the n , the larger the curvature. A similar effect occurs when Δr is increased. Figure 2 also shows the results of a network of random sinuous pores. The randomness is introduced by choosing n for each pore from a uniform PD between 1 and 200 and it does not remove the curvature in the σ vs σ_f plot. Thus, geometry alone (without the interplay of clay chemistry) is sufficient to produce nonlinear effects. Λ and c for the 3D sinuous pore network are shown in Table I. For all the cases studied, $c \sim 1$ and therefore Λ is a proper measure of the length scale governing k .

Are there any geometries for which c is *not* close to 1? Consider the case of a system near its percolation threshold. If all the occupied tubes have the same radius, then $c \equiv 1$.³ Suppose, however, that the occupied tubes are taken from a PD which is a power law; such distributions model continuum percolation¹¹ and are known to change the transport exponents in nonuniversal ways. To analyze this problem we use the hierarchical model for the percolation backbone⁶ of Fig. 1(b). This model is designed to incorporate the nodes-blobs-links structure of the backbone. We take each bond in the basic unit to represent a cylinder of radius r chosen from a PD $P(r)$ behaving as r^{a-1} for $r \rightarrow 0$ (all cylinders have the same length l). Since $\Lambda = r$, $g_e \sim r^2$, and $g_h \sim r^4$, the PD's for these quantities are given by power laws with the exponents $\alpha_\Lambda = a$, $\alpha_e = a/2$, and $\alpha_h = a/4$, respectively. The four interior

TABLE I. Λ and c for 3D cubic pore networks. $[r_1, r_2]$ refers to a uniform distribution between r_1 and r_2 . ISP (RSP) denotes identical (random) sinuous pores.

Bond	Pore radii distribution	Λ	c
Single tube	[0,1]	0.61	1.37
Single tube	[1,2]	1.53	1.09
Double tubes	[0,1], [0,1]	0.46	1.40
Double tubes	[0,1], [1,2]	0.67	1.26
Double tubes	[0,1], [100, 200]	0.61	1.37
ISP-100 tubes	...	0.27	0.82
ISP-1000 tubes	...	0.28	0.81
RSP	...	0.27	0.81

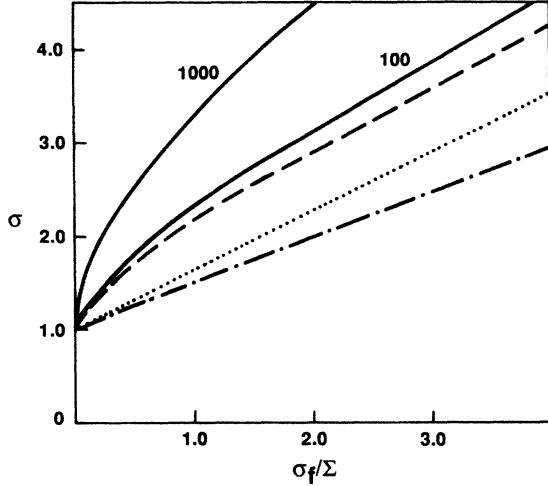


FIG. 2. Normalized electrical conductivity of the 3D network, $\sigma(\sigma_f; \Sigma)/\sigma(0; \Sigma)$ vs the fluid conductivity σ_f for surface conductivity $\Sigma=0.5$. Dotted line, random network of single tubes. Dotted-dashed line, random network of double tubes. Solid line, uniform network of sinuous pores with the number of layers as indicated. Dashed line, random network of sinuous pores with 100 layers on an average.

sites of the basic unit in Fig. 1(b) are decimated out to obtain an effective Λ , g_e , and g_h between the end sites. We represent the physical quantities such as Λ , g_e , and g_h generically as J and study the scaling of $J(L)$,

$$J(L) \sim L^{y_p} \sim L_1^{y_p}, \quad (3)$$

where $J(L)$ is the "coupling" J for a sample of linear size L , $L_1 \sim L^{1/y_p}$ is the number of "red" bonds at length scale L (Ref. 12) (a red bond is one whose removal cuts the backbond into two pieces¹³), and v_p is the correlation length exponent at the threshold. Our results for $(v_p y_p)^{-1}$ are shown in Table II. The results for g_e and g_h are obtained by noting that the conductance problem maps onto the Heisenberg ferromagnet and that both problems have been studied before.^{11,14,15} The new ingredient is that α_e and α_h are different. The Λ problem may be solved following the treatment in Ref. 15. The result is that (analogous to the Ising ferromagnet¹⁵) the blobs do not play any role and it is only the "red" bonds that contribute leading effectively to a 1D problem. The recursion relation for the unit of Fig. 1(b) is

$$\frac{1}{\Lambda'} = \frac{\Lambda_5 + \Lambda_6}{\Lambda_5^2 + \Lambda_6^2} + c_1 - A/B, \quad (4)$$

where

$$\begin{aligned} c_k &= \sum_{i=1}^4 \Lambda_i^{-k}, \quad k=1,2,3, \\ A &= c_1 + c_2(\Lambda_5 + \Lambda_6) + (c_1 c_2 - c_3)(\Lambda_5^2 + \Lambda_6^2), \\ B &= 1 + c_2(\Lambda_5^2 + \Lambda_6^2). \end{aligned}$$

We have analyzed this recursion relation, as in the studies of the 3D network. The initial pool of Λ 's are selected

TABLE II. Results for the exponent $[-(v_p y_p)^{-1}]$ for the electrical conductance, the hydraulic conductance, and Λ for the model of the percolation backbone (Ref. 6) in d dimensions. $\alpha_c = \ln[8/(6-d)]/\ln[8/(6-d)+1/2]$, $2 \leq d \leq 6$.

J	$-1/(v_p y_p)$
g_e	$\min(\alpha_e, \alpha_c)$
g_h	$\min(\alpha_h, \alpha_c)$
Λ	α_Λ

from a PD $P_0(\Lambda) \sim \Lambda^{\alpha-1}$ in the $\Lambda \rightarrow 0$ limit. Upon iteration, the PD acquires a fixed shape and it narrows by a factor $4^{-1/\alpha}$ with each iteration in accord with Table II.

To understand these results, consider the case when all the Λ 's are widely separated. Equation (4) then reduces to $\Lambda' = \min[\Lambda_1, \Lambda_2, \Lambda_3, \Lambda_4, \max(\Lambda_5, \Lambda_6)]$ showing the irrelevance of the blobs. It is also useful to consider the recursion relation for two tubes in parallel (series) with Λ values of Λ_5 and Λ_6 (Λ_1 and Λ_2):

$$\Lambda_{\text{parallel}} = \frac{\Lambda_5^2 + \Lambda_6^2}{\Lambda_5 + \Lambda_6} = \frac{\langle \Lambda^2 \rangle}{\langle \Lambda \rangle} \quad (5)$$

and

$$\Lambda_{\text{series}} = \frac{\Lambda_1 \Lambda_2 (\Lambda_1^2 + \Lambda_2^2)}{\Lambda_1^3 + \Lambda_2^3} = \frac{\langle \Lambda^{-2} \rangle}{\langle \Lambda^{-3} \rangle}. \quad (6)$$

When Λ_5 and Λ_6 are both picked from a PD with an exponent α , then it is straightforward to show that $P(\Lambda_{\text{parallel}}) \sim \Lambda_{\text{parallel}}^{2\alpha-1}$ for $\Lambda_{\text{parallel}} \rightarrow 0$. In the series case, when Λ_1 and Λ_2 are characterized by exponents α_1 and α_2 (unlike the parallel case, the series case does not necessarily have $\alpha_1 = \alpha_2$; a blob can be series with a "red" bond), Λ_{series} can be shown to follow the distribution $P(\Lambda_{\text{series}}) \sim \Lambda_{\text{series}}^{\min(\alpha_1, \alpha_2)-1}$ again showing that the blob contributions are irrelevant.

Using the results of Table II, the scaling behavior of c defined in Eq. (2) is $c(L) \sim L^{y_p} \sim L_1^{y_p}$ with

$$v_p y_p = 2/\alpha + \max\left\{\frac{2}{\alpha}, \frac{1}{\alpha_c}\right\} - \max\left\{\frac{4}{\alpha}, \frac{1}{\alpha_c}\right\}.$$

Remarkably, for $\alpha = \infty$ (a gap at the origin in the PD of r) and $\alpha < 2\alpha_c$, $c(L)$ is scale invariant. For $\alpha > 4\alpha_c$, $v_p y_p = 2/\alpha$ but for $2\alpha_c < \alpha < 4\alpha_c$, $v_p y_p = 1/\alpha_c - 2/\alpha > 0$. For the Swiss cheese (inverted Swiss cheese) model¹¹ in 3D, $\alpha_e = \frac{2}{3}$, $\alpha_h = \frac{2}{7}$, $\alpha_\Lambda = 1$ ($\alpha_e = 2$, $\alpha_h = \frac{2}{3}$, $\alpha_\Lambda = 2$) leading to scale invariance (no scale invariance) of c .

Using finite size scaling,⁷ the derived exponents may be related to percolation exponents in the limit $p \rightarrow p_c$: $\sigma \sim (p - p_c)^\nu$, where σ denotes the conductivity defined by $J \sim \sigma L^y$ for the $p=1$ (no dilution) case with $t = y v_p - v_p y_p$, $y_e = d - 2$, $y_h = d - 2$, and $y_\Lambda = 0$.

One of us (M.C.) acknowledges the support of the National Science Foundation through Grant No. DMR-8553271.

*On leave from Institute of Theoretical Physics, Warsaw University, 00-681 Warsaw, Poland.

†Present address: Department of Physics and Astronomy, University of Massachusetts, Amherst, MA 01003.

¹See, for example, *Physics and Chemistry of Porous Media*, edited by D. L. Johnson and P. N. Sen, AIP Conference Proceedings, No. 107 (American Institute of Physics, New York 1984); *Physics and Chemistry of Porous Media II*, edited by J. R. Banavar, J. Koplik and K. W. Winkler, AIP Conference Proceedings, No. 154 (American Institute of Physics, New York, 1987).

²D. L. Johnson, J. Koplik, and L. M. Schwartz, *Phys. Rev. Lett.* **57**, 1564 (1987).

³D. L. Johnson, J. Koplik, and R. Dashen, *J. Fluid Mech.* **176**, 379 (1987).

⁴J. R. Banavar and D. L. Johnson, *Phys. Rev. B* **35**, 7283 (1987); see also A. J. Katz and A. H. Thompson, *ibid.* **34**, 8179 (1986), for another definition of the the relevant length scale.

⁵S. R. Baker and I. Rudnick, *IEEE Trans. UFFC* **33**, 118 (1986); D. L. Johnson, T. J. Plona, and H. Kojima, in *Physics and Chemistry of Porous Media II*, Ref. 1.

⁶L. de Arcangelis, S. Redner, and A. Coniglio, *Phys. Rev. B* **31**, 4725 (1985); Fig. 1(b) shows the model for a percolation backbone in $d=4$; our results are easily generalized to any d .

⁷See, for example, M. N. Barber, in *Phase Transitions and Critical Phenomena*, edited by C. Domb and J. L. Lebowitz (Academic, New York, 1983), Vol. 8.

⁸M. H. Waxman and L. J. M. Smits, *Soc. Pet. Eng. J. Trans. AIME*, **243**, 107 (1968); C. Clavier, G. Coates, and J. Dumanoir, *Soc. Pet. Eng. J.* **24**, 153 (1984); W. C. Chew and P. N. Sen, *J. Chem. Phys.* **77**, 2042 (1982).

⁹P. N. Sen and R. Kan, *Phys. Rev. Lett.* **58**, 778 (1987); R. Kan and P. N. Sen, *J. Chem. Phys.* **86**, 5748 (1987).

¹⁰See, for example, S. Kirkpatrick, *Phys. Rev. B* **15**, 1533 (1977); B. W. Southern and A. P. Young, *J. Phys. C* **10**, 2179 (1977).

¹¹B. I. Halperin, S. Feng, and P. N. Sen, *Phys. Rev. Lett.* **54**, 2391 (1985); S. Feng, B. I. Halperin, and P. N. Sen, *Phys. Rev. B* **35**, 197 (1987).

¹²A. Coniglio, *J. Phys. A* **15**, 3829 (1982).

¹³H. E. Stanley, *J. Phys. A* **10**, L211 (1977); A. Coniglio, *Phys. Rev. Lett.* **46**, 250 (1981).

¹⁴P. M. Kogut and J. P. Straley, *J. Phys. C* **12**, 2151 (1979); A. Ben-Mizrahi and D. J. Bergman, *ibid.* **14**, 909 (1981); J. P. Straley, *ibid.* **15**, 2333 **15**, 2343 (1982); J. Machta, R. A. Guyer, and S. M. Moore, *Phys. Rev. B* **33**, 4818 (1986).

¹⁵J. R. Banavar, A. J. Bray, and S. Feng, *Phys. Rev. Lett.* **58**, 1463 (1987).